Improved BRDF metrology platform for Copernicus CO2I FCU calibration

E. Mazy *, C. Michel, J. Hastanin, L. Clermont, L. Rossi, C. Dandumont, M. Georges, S. Marcotte and C. Thizy

Centre Spatial de Liège (CSL), Space sciences, Technologies and Astrophysics Research (STAR) Institute, Université de Liège, Liege Science Park, Angleur, B-4031, Belgium

ABSTRACT

Copernicus CO2M is a satellite mission designed for high precision and accuracy mapping of atmospheric carbon dioxide emission sources resulting from anthropogenic activities. The Centre Spatial de Liège (CSL) is responsible for designing and implementing the Flight Calibration Unit (FCU) dedicated to in-flight spectral and radiometric calibration of the CO2I spectroscopic instrument, including the calibration of its main optical components, such as reference diffusers (referred to as solar diffuser standards). The ambitious target sensitivity of the CO2I instrument necessitates an unprecedented level of precision and accuracy in solar diffuser standards calibration. This also requires a low level of stray light, achieved through optical baffling. In this paper, we address key issues related to the optical calibration of FCU diffuser standards, including the engineering aspects of its practical implementation. In particular, we present an original instrumental platform developed by our research group for high-precision measurement of the Bidirectional Reflectance Distribution Function (BRDF) of FCU diffuser standards. Additionally, we report and discuss results of experimental investigations of the presented instrumental approach.

Keywords: BRDF measurement, Flight Calibration Unit, FCU, diffuser calibration, Copernicus CO2M

* emazy@uliege.be

1. INTRODUCTION

Copernicus CO2M is a satellite mission designed for high precision and accurate mapping of atmospheric carbon dioxide emission sources resulting from anthropogenic activity. The space segment of the CO2M mission is foreseen to be implemented as a constellation of identical satellites. Each satellite will carry a push-broom imaging spectrometer, known as the CO2 imager (CO2I), as part of its main payload. This spectrometer will operate in three spectral bands: one in the Near Infrared (NIR) and two in the Short-Wave Infrared (SWIR) spectral ranges (NIR: 747-773 nm; SWIR1: 1590-1675 nm; SWIR2: 1990-2095 nm) [1]-[2].

In the context of the Copernicus CO2M project, the Centre Spatial de Liège (CSL) is responsible for the design, manufacturing, verification, calibration, and delivery of the Flight Calibration Unit (FCU) for in-flight calibration of the CO2I instrument. This includes the mechanism and optical calibration components, such as reference diffusers and internal light sources for WLS (White Light Source) and ISRF (Instrument Spectral Response Function) calibration, as well as the control electronics (FCU-E).

The FCU is positioned in front of the CO2I instrument telescope. The standard procedure for the on-board calibration of the CO2I instrument comprises three basic operating modes: "*Earth observation*", "*Sun calibration*", and "*Dark calibration*." In Earth observation mode, light enters through the Earth Port (EP) of the FCU and is transmitted directly to the telescope. In Sun calibration mode, sunlight enters through the Sun Port (SP) and, after scattering on a reference diffuser (the so-called solar diffuser standard), is directed toward the entrance aperture of the telescope. In Dark calibration mode, both the Sun and Earth ports are closed using a shutter to conduct internal noise tests.

A correct understanding of the dynamics of atmospheric CO2 concentrations, including anthropogenic contributions, requires very high precision and accuracy in the CO2I in-flight calibration. Therefore, detailed knowledge of the Bidirectional Reflectance Distribution Function (BRDF) [3]-[4] of the solar reference diffusers is essential. In this context, it is worth noting that, according to the requirements of the CO2I FCU specification, the absolute BRDF of the

Optical Measurement Systems for Industrial Inspection XIV, edited by Peter Lehmann, Wolfgang Osten, Armando Albertazzi Gonçalves, Proc. of SPIE Vol. 13567
1356719 · © 2025 SPIE · 0277-786X · doi: 10.1117/12.3059481

FCU must be known for the nominal incidence configuration with an accuracy better than 0.6% at the 95% confidence level over the entire wavelength range of interest (NIR, SWIR1, and SWIR2). All other angular configurations should be known with an accuracy better than 1%@2σ for VIS and NIR, and 2%@2σ for the SWIR1 and SWIR2 spectral bands. Accordingly, the ambitious target sensitivity of the CO2I instrument necessitates a very high level of precision and accuracy in solar diffuser standards calibration, thus requiring the use of a high-precision BRDF measuring bench.

The CSL optical metrology team has been involved for 15 years in the pre-launch laboratory characterization of the solar diffuser standards dedicated to in-flight spectral and radiometric calibration of spectrometers onboard Earth observation satellites [5]-[8]. . In our work, BRDF metrology is typically conducted on a robot-based gonioreflectometer (RG) bench developed by our research team [9]-[11]. The high accuracy and precision of this metrology bench has been experimentally demonstrated in several projects undertaken in collaboration with ESA. However, our recent studies have shown the potential for further enhancing the precision of this bench in the SWIR spectral ranges by utilizing supercontinuum light sources (also known as white light lasers).

In this paper, we address key issues related to the optical calibration of FCU diffuser standards, including the engineering aspects of its practical implementation. Specifically, we present an original instrumental platform developed by our research group for high-precision measurement of the BRDF of CO2I FCU diffuser standards. The measurement bench described in this article enables high-precision BRDF measurements across an extended spectral range from 400 nm to 2200 nm, meeting all the aforementioned requirements of the CO2I FCU specification.

Additionally, we report and discuss some results of experimental investigations into the presented instrumental approach.

2. BACKGROUND

The BRDF is a multidimensional function determining the amount of light reflected from a diffuse surface. It is defined as the ratio of the directional reflected radiance (dL) to the directional incident irradiance (dE) and can be calculated as follows, [9]-[11]:

$$BRDF(\theta_i,\phi_i,\theta_r,\phi_r,\lambda) = \frac{dL_r(\theta_i,\phi_i,\theta_r,\phi_r,\lambda)}{dE_i(\theta_i,\phi_i,\lambda)} = \frac{dL_r(\theta_i,\phi_i,\theta_r,\phi_r,\lambda)}{L_i(\theta_i,\phi_i,\lambda)\,d\Omega_r\cos(\theta_i)} \quad \left[sr^{-1}\right] \tag{1}$$

where λ is the wavelength of the incident light, $d\Omega_r$ denotes the solid angle of the detection aperture, θ_i and φ_i are respectively elevation and azimuth angles of the incident beam and θ_r and φ_r the ones of the scattered beam, as illustrated in Fig. 1; dL_r and dE_i denote respectively the differential reflection radiance and the differential incident irradiance.

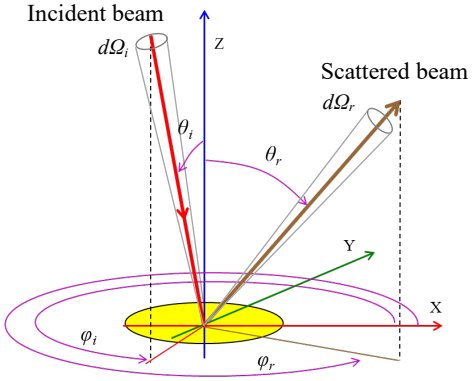

Figure 1. Geometry for the definition of the BRDF

In the case of a real BRDF bench, the differential terms in this equation cannot be measured directly. Instead, the direct measurements focus on the value of the BRDF averaged over the illuminated surface of the sample, viewed within the detector's solid angle of view. This averaged BRDF is then calculated as follows:

$$\left\langle BRDF(\theta_i,\phi_i,\theta_r,\phi_r,\lambda)\right\rangle = \frac{S_{scat}(\theta_i,\phi_i,\theta_r,\phi_r,\lambda)}{S_{src}} \cdot \frac{1}{d\Omega_r\cos(\theta_i)} \tag{2}$$

In this equation, S_{scat} and S_{src} are respectively the scattering and reference signals measured in required angular configuration (θ_i, φ_i; θ_r, φ_r) in spectral band of interest.
Additionally, for a realistic BRDF measuring bench, some extra terms associated with its design features and the measurement method used should be introduced into this equation. In this context, the equation above can be rewritten as follows:

$$\left\langle BRDF(\theta_i,\phi_i,\theta_r,\phi_r,\lambda)\right\rangle = \frac{S_{scat}(\theta_i,\phi_i,\theta_r,\phi_r,\lambda)}{S_{src}} \cdot \frac{1}{d\Omega_r \cos(\theta_i)} \cdot \prod_n F_n(\theta_i,\phi_i,\theta_r,\phi_r,\lambda) \tag{3}$$

In this equation, F_n refers to the so-called 'correction factors' introduced to account for the effects of various systematic errors inherent in the bench used for the BRDF measurement results.
One of the correction factors most commonly used in practice is the uniformity correction factor F_{unif} , which was introduced to address the spatial non-uniformity of the incident beam irradiance distribution on the surface of the diffuser under test (DUT). Additionally, it's important to mention the correction factors that account for the effects associated with stray light, the nonlinearity of the detector response, and so on.
In the case of the CO2M FCU project, the calibration plan requires that the DUT be calibrated against standard reference samples (SRS) with known BRDF, specifically standard diffusers certified by independent national metrology standards laboratories such as NIST (US National Institute of Standards and Technology) and/or PTB (Physikalisch-Technische Bundesanstalt). Here, the BRDF of the DUT is defined as:

$$\begin{aligned}\left\langle BRDF_{Abs}^{diffuser}(P,\lambda)\right\rangle = {} & \frac{S_{diff}(P_{diff},\lambda)}{S_{sample}\left(P_{ref.sample},\lambda\right)} \cdot \frac{\cos\left(\theta_i\left(P_{ref.sample}\right)\right)}{\cos\left(\theta_i\left(P_{diff}\right)\right)} \cdot BRDF_{Abs}^{Sample}(P_{ref.sample},\lambda) \times \\ & \times \frac{S_{sample.mon}\left(P_{ref.sample},\lambda\right)}{S_{diff.mon}(P_{diff},\lambda)} \cdot \frac{F_{unif}(P_{diff},\lambda)}{F_{unif}\left(P_{ref.sample},\lambda\right)}\end{aligned} \tag{4}$$

, where $BRDF_{Abs}^{Sample}(P_{ref.sample},\lambda)$ is the BRDF as provided in calibration certificate of the SRS; the terms S and F denote the measured signals and beam uniformity correction factors, respectively; the terms P denote angular configurations, for which BRDF measurements are performed (i.e., combinations of the four angles $(\theta_i, \varphi_i; \theta_r, \varphi_r)_{diff}$ and $(\theta'_i, \varphi'_i; \theta'_r, \varphi'_r)_{ref.sample}$).
In this equation, the subscripts 'diff.' and 'ref. sample' respectively label the terms related to the DUT and SRS data, while the subscript 'mon' labels the reference signals measured by a dedicated measurement system known as the "source monitoring system" (SMS). The reference signal measured by this system, also referred to as the 'monitoring signal,' is used in the presented metrological approach to eliminate the contribution of uncontrollable fluctuations in the power of the light source system from the measurement data.
It is important to note that, in the case of the CO2M project, along with the BRDF absolute value, the calibration plan for the CO2I FCU diffuser standards also specifies the measurement of their relative angular BRDF. This measurement is used to develop a multiparameter Rahman angular model of the BRDF ([23]) for the solar reference diffusers under test. The relative angular BRDF is defined, in the same notation as in the equations above, as follows:

$$\left\langle \mathrm{Rel}_{ang}(P,P_{ref},\lambda)\right\rangle = \frac{S_{diff}(P,\lambda)}{S_{diff}\left(P_{ref.},\lambda\right)} \cdot \frac{S_{diff.mon}\left(P_{ref},\lambda\right)}{S_{diff.mon}(P,\lambda)} \cdot \frac{\cos\left(\theta_{iref}\right)}{\cos\left(\theta_i\right)} \cdot \frac{F_{unif}(P,\lambda)}{F_{unif}\left(P_{ref},\lambda\right)} \tag{5}$$

In this equation, the subscript 'ref.' labels the terms related to the measurement data for the reference angular configuration.
In our work, we use the modified empirical Rahman angular model, for which fine fitting is conducted using an additional polynomial term $F'(P,k_{ij})$ added to the basic Rahman equation:

$$\mathrm{BRDF}(P,\lambda) = \rho_0 \cdot M\left(P,k\right) \cdot F\left(g\left(P\right),\Theta\right) \cdot \left(1+R\left(G\left(P\right),\rho_1\right)\right) + F'\left(P,k_{ij}\right) \tag{6}$$

In this equation, the terms $M(P,k)$ and $F(g(P),\Theta)$ denote, respectively, the Minnaert and the Henyey-Greenstein functions; G is the geometric factor; the term $(1+R(G(P)), \rho_1)$ characterizes the hot-spot effect; ρ_0, ρ_1, k, Θ are fitting parameters of the basic Rahman model (for a more detailed explanation of the terms of the Rahman BRDF angular model, see [23]).

Finally, it should be noted that, in the case of the BRDF bench presented in this paper, the wavelength selection and tuning in the NIR/SWIR ranges are performed using Acousto-Optic Tunable Filters (AOTF). Accordingly, the light beams emitted by the supercontinuum light source, depending on the requirements of the intended measurement test campaign, may be fully polarized or unpolarized.
In the case of measurements involving a polarized light beam, the total BRDF can be calculated as follows:

$$\left\langle BRDF_{Abs}^{diffuser}(P,\lambda)\right\rangle = \frac{\left\langle BRDF_{Abs}^{diffuser}(P,\lambda)\right\rangle_p + \left\langle BRDF_{Abs}^{diffuser}(P,\lambda)\right\rangle_s}{2} \quad (7)$$

In this equation, the indices *p* and *s* denote the two basic polarization states for which BRDF measurements of the diffuser under test were performed.

3. MEASUREMENT BENCH DESIGN AND OPERATION PRINCIPLE

As noted above, the BRDF measurement bench used in our experimental work was developed on the basis of the existing robot-based gonio-reflectometer bench, which was also developed by our research team within the framework of previous research projects, [9]-[11].

The developed CSL BRDF measurement bench is depicted in Fig.2 and Fig.3.

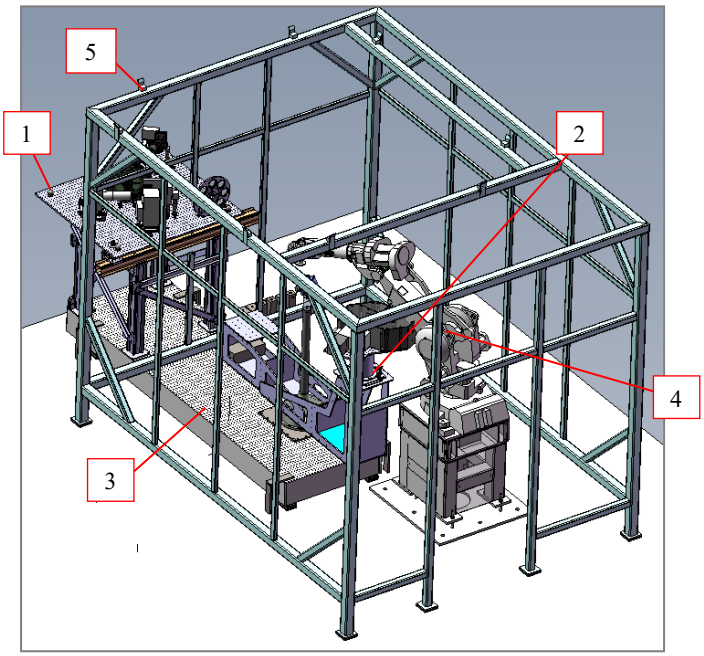

Figure 2. Robot-based BRDF measurement bench (without the black walls of the class 100)

This bench features a light source assembly (1) and a detector assembly (2) mounted on a honeycomb optical bench (3), along with a robotic manipulator (4) designed to position the sample for testing at angular orientations that correspond to the required measurement configuration (θ_i, φ_i; θ_r, φ_r) and maintain that position during measurements.

The entire metrology bench, except for the light source assembly, is located in a large volume clean room, referred to as a black tent, which provides high isolation from light interference. The black tent features a supporting structure (5) with straylight absorbing black panels (not shown in Fig.2 for clarity). The clean room is outfitted with standard laminar air flow systems to maintain the required level of environmental cleanliness. The source assembly is positioned outside the black tent to ensure accessibility.

The detector assembly (2) includes a detector optical system (6) mounted on a motorized rotation stage (7) that moves it around a fixed vertical axis (see Fig. 3). The rotation stage consists of a RV350 stage from Newport with a stepper motor. Its angular resolution is approximately 0.001°.

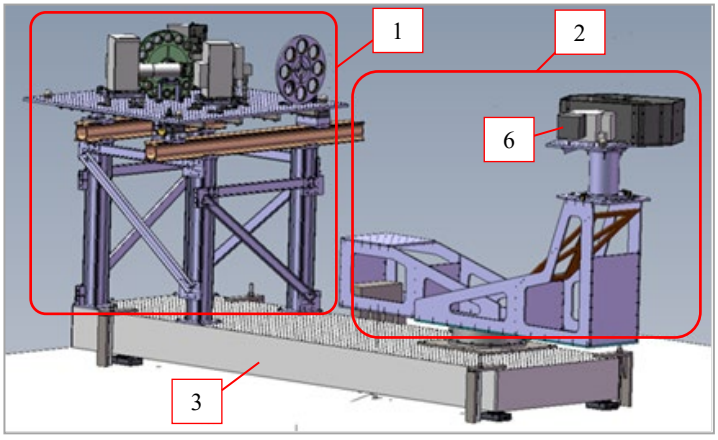

Figure 3. Robot-based BRDF measurement bench (without the black walls of the class 100):

The optical detector system (6) is shown in Fig. 4. It essentially comprises an off-axis parabolic (OAP) mirror (1), a pinhole assembly (2), an integrating sphere (3), a relay optical system (4), an attenuator wheel, and a VIS-NIR or SWIR detector (6). In the described setup, the detector optical system (6) features a thermoelectrically cooled Si photodiode with an integrated preamplifier from 'Hamamatsu' as the VIS-NIR detector, and an InGaAs photodiode from 'Hamamatsu' as the SWIR detector. Both are utilized in conjunction with a lock-in amplifier (SR830 from 'Standford Research System').

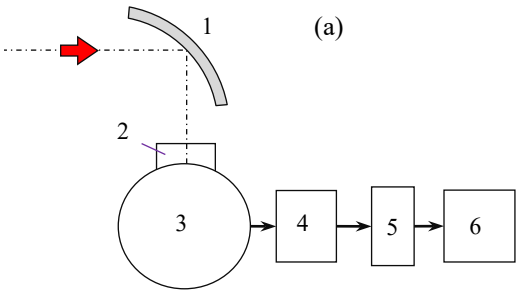

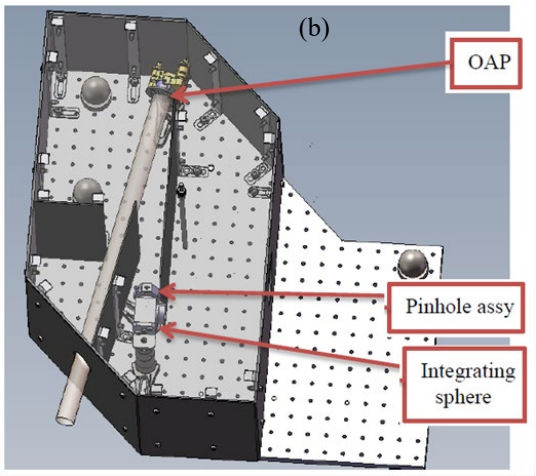

Figure 4. The detector optical system in absolute mode configuration: (a) schematic functional diagram, (b) 3D CAD model

The detector optical system is designed to operate in four basic measurement configurations: two configurations for conducting absolute BRDF measurements using either a VNIR or SWIR detector, and two configurations for conducting relative BRDF measurements, also using either a VNIR or a SWIR detector. In the relative BRDF measurement configurations, the VNIR or SWIR detector (6) is positioned directly at the output of the detector assembly integrating sphere (3) output port, while the attenuator wheel (5) and relay optics (4) are removed.

As noted above, the introduction of a supercontinuum light source resulted in a significant increase in the accuracy and precision of the presented CSL BRDF metrology bench in the NIR and SWIR wavelength ranges.

It is worth noting that further improvements in the quality of BRDF measurements were also achieved through engineering optimization of various modules and subsystems of this bench, as well as advancements in the data

processing method. However, in this article, for the sake of brevity, a discussion of these improvements is omitted (the main issues related to this engineering optimization, as well as detailed explanations of the developed data processing, will be published in a forthcoming paper).

In the developed BRDF measurement bench, the light source assembly consists of two optical sub-systems (see Fig. 5): a light source featuring a 300 W Xenon arc lamp designed for measurements in the VIS wavelength range (400 – 500 nm) and a supercontinuum light source (denoted as SK in Fig. 5) intended for measurements in the NIR and SWIR wavelength ranges. Consequently, the light source assembly supports two operating modes: Xe light mode and the supercontinuum mode. The selection of mode depends on the project, and modifications are performed manually.

Compared to conventional broadband light sources, such as Xenon arc lamps, supercontinuum sources offer significantly higher output light beam intensity in the NIR/SWIR spectral ranges. This results in a notably improved signal-to-noise ratio when measuring the sample BRDF in these spectral ranges. Therefore, utilizing supercontinuum light sources can significantly enhance the accuracy and precision of BRDF measurement results, as well as reduce the overall duration of BRDF measurement (since a significant increase in the signal-to-noise ratio allows for a reduction in integration time).

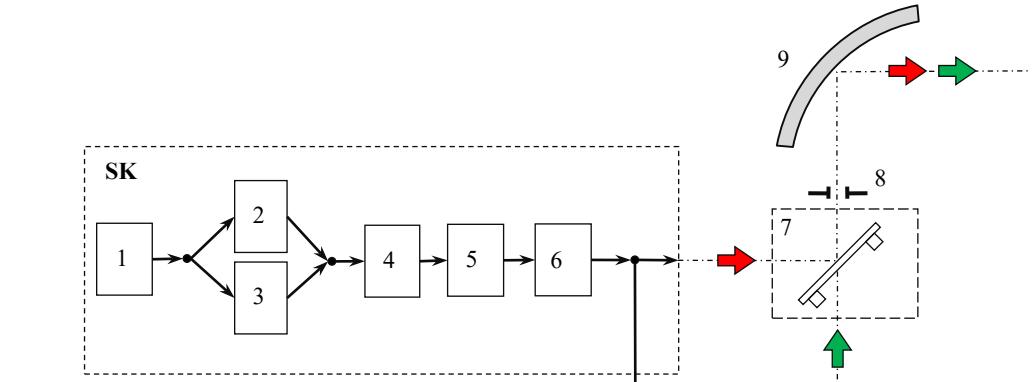

1- Primary supercontinuum light source
2- AOTF NIR
3- AOTF SWIR
4- Filter wheel assembly (NIR/SWIR)
5- Optical chopper
6- Polarization state selector
7- Free space speckle reducer
8- Pinhole assembly
9- Output collimator
10- Xenon arc lamp
11- Collimating system
12- Filter wheel assembly (VIS)
13- Beam chopper
14- SMS optical system
15- Integrating sphere
16- VNIR detector module
17- SWIR detector module

Figure 5. Schematic functional diagram of the light source assembly

The supercontinuum light source (SK) includes a primary supercontinuum light source (1), a wavelength selector system built on two AOTFs designed to operate in the NIR and SWIR spectral bands — a NIR AOTF (2), a SWIR AOTF (3), a filter wheel (4) equipped with a set of dedicated optical filters to reduce the amount of stray spectral light in the system, an optical chopper (5), a polarization state selector (6), and a speckle reducer (7). These functional modules are based on commercially available components (see Table 1).

Table 1. Commercially available components involved in the SK light source assembly

#	Component assembly	Provider	Ref./Name
1	Primary light source	YSL photonics	SC-OEM (430-2400 nm @ 8W@ 5MHz)
2	NIR AOTF	YSL photonics	AOTF-PRO
3	SWIR AOTF	YSL photonics	AOTF-SWIR
4	Filter wheel	THORLABS	FW102C
5	Optical Chopper	ORIEL	75160NF
6	Polarization state selector	THORLABS	Half-wave retarder SAHWP05M -700 (for NIR)
		THORLABS	Half-wave retarder SAHWP05M -1700 (for SWIR)
7	Speckle reducer	DYOPTIKA	Phase-randomizing deformable mirror
8	Pinhole assembly	VIAVI Solution	EDC -20 -G-1R diffuser
9	Output collimator	Optical Surface	Off-axis parabolic mirror (f=326.7mm@D=101.6mm)

The primary supercontinuum light source (1) emits light within the wavelength range of 430-2400 nm with an average power of 8 W. The operating wavelength is selected using the corresponding AOTF (NIR or SWIR). It is important to note that the light beam at the output of the AOTF is linearly polarized, according to its working principle. Therefore, to facilitate the measurement of the sample BRDF for two independent orthogonal polarizations, a polarization state selector (6) employing two dedicated half-wave retarders is integrated into the optical system.

The VIS light source assembly includes a 300W Xenon arc lamp source (10) from Oriel with feedback control, a collimating/focalizing system (11), a filter wheel assembly (12) featuring two filter wheels equipped with band-pass filters for spectral selection, and a beam chopper (13) from Newport-Oriel.

The VIS light source was developed as part of our previous work; a more detailed description of its operational principle and performance parameters can be found in our publications [9]-[11]. It is only worth noting that the light beam at the output of the VIS light source is not polarized.

The light beams emitted by both the SK and VIS light sources, after passing through the free space speckle reducer (7), are projected onto the pinhole (8) and then collimated using the output collimator (9) based on an off-axis parabolic mirror (f=326.7 mm @ D=101.6 mm). The pinhole assembly consists of a black-coated pinhole with a diameter of 3 mm and one dedicated diffuser from VIAVI Solutions.

The source monitoring system (SMS) comprises a dedicated SMS optical system (14), which diverts part of the light source output beam and directs it to one of the detectors according to the selected spectral range (VNIR or SWIR). It includes an integrating sphere (15) from Labsphere and two detector modules (16) and (17): a Si photodiode with a transimpedance amplifier from Newport for VNIR and an InGaAs photodiode from Judson for SWIR spectral ranges, respectively. The reference signal, measured in-situ by this system (also referred to as the 'monitoring signal'), is used to filter out the effects of uncontrollable fluctuations in the output power of the light source assembly (caused by thermal fluctuations, supply voltage variations, etc.) from the BRDF measurement data.

The complete FCU instrument consists of a rotating multi-functional barrel (1) (i.e., a rotor), a stator (4), a Sun baffle (2) and a pupil baffle (3). It shares similarities with a past project of our institute, the Sentinel-4 UVN instrument, for which a similar in-flight calibration units had been developed [7]-[8]. For these systems, it is important that stray light be controlled by the baffle to ensure optical radiometric accuracy with the calibration, which can be done with a dedicated test [8][12][13]. While numerical methods have been recently developed to remove stay light by post-processing [14]-[20], these are not appropriate for application in a calibration unit. Optimal design and black treatment is therefore a prerequisite [21]-[22].

For mass purposes, the measured FCU is limited and includes a rotating multi-functional barrel (1) that houses the diffusers under test (DUT), a dummy limited Sun baffle (2) through which the light enters and travels before reaching the DUT, and a pupil flange (3) that allows the scattered light to exit from the FCU mechanism and pass to the detector system. The alignment of the barrel (4) of the FCU mechanism on the measurement bench is performed using a system of laser tracker targets (LTT) that represent the mechanical reference frames of the mechanism. The FCU mechanism is configured to the required measurement setup and maintained in this position during the BRDF measurements by a 6-axis robotic manipulator (5) ABB IRB 2400/16. The robot manipulator used in the presented instrumental bench provides an angular accuracy of 0.005° and a spatial accuracy of 0.03 mm.

It is important to note that the robotic manipulator is subject to a relatively high mechanical load from the FCU mechanism, which results from the comparatively large mass and size of the latter. Consequently, special care has been

devoted in our work to addressing the accuracy and precision of the tested diffusers' alignment, as well as the mechanical stability issues of the measurement system. As a result of the engineering optimization of the mechanical part of the presented BRDF bench, the contribution of uncertainty related to the FCU mechanism alignment error to the overall error budget in the so-called 'Nominal' angular configuration (θi=48.57°, φi=9.46 °, θr=54° and φr=180°) was reduced to 0,017% for the FCU nominal and redundant diffusers.

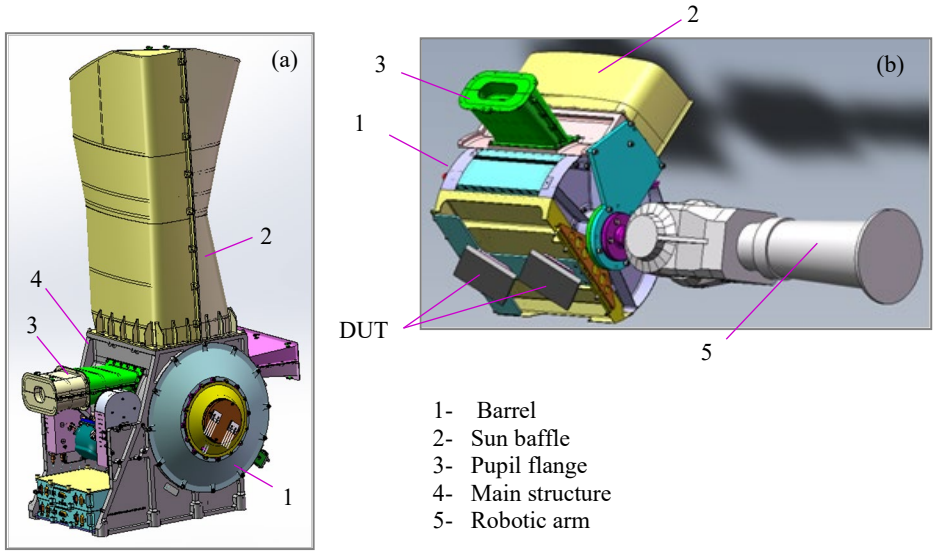

Figure 6. FCU mechanism (3D CAD models): (a) general view; (b) an exploded-view drawing of the barrel-baffles assembly and mechanical interfacing with the robotic arm.

In principle, the presented BRDF bench can be utilized in two primary measurement modes: absolute BRDF measurements and relative (angular/spatial) BRDF measurements.

In the former mode, the BRDF measurement procedure involves two consecutive measurements: the reference and scattered beam measurements. During the reference measurement, the sample under test is removed from the optical path between the source and the detector, while the detector assembly is moved in front of the incident light beam. To measure the scattered beam power, the sample under test is reinstalled in its original position, and then both the sample and detector are positioned to the required angular configuration. The BRDF value is then calculated by substituting the measured values of the reference and scattered signals into Eqs. (1-3).

In the case of the latter relative measurement mode, the BRDF of the sample being tested at various angular and spatial configurations is measured without removing the sample from the optical path between the source and the detector. More precisely, the BRDF value for a specific angular/spatial configuration is calculated from the intensity of the scattering signal measured in this configuration and the a priori known BRDF values for certain reference samples and/or measurement configurations (see Eqs. 4-5).

As noted above, the CO2M FCU calibration plan requires that the solar DUT be calibrated against standard reference diffusers certified by independent national metrology standards laboratories (PTB and NIST), where the absolute BRDF is known a priori. In other words, the BRDF measurement procedure implemented within the CO2M FCU project includes two consecutive measurements of scattering signal intensity: first for the certified reference diffuser and then for the solar DUT. The measurement of scattering signal intensity for both the reference diffuser and the solar DUT is carried out in the same measurement configurations. The BRDF of the solar DUT is then determined by substituting the values of scattering signal intensity measured for both diffusers and the absolute BRDF of the certified reference diffuser (provided by PTB and/or NIST) into Eq. (4).

In this work, we used Lambertien-like diffusers 'white Zenith' from SPHEREOPTICS as a reference sample, which were previously characterized at NIST, PTB, and CSL on the robot-based high precision gonioreflectometer.

The relative method of BRDF measurement described above is preferred because it reduces overall measurement time and avoids issues related to the impact on the total error budget stemming from measurement system instability, stray light, residual fluctuations in light source intensity, noise in detectors, and readout electronics, among others. In this context, it is important to note that, according to the CO2M FCU calibration plan requirements, the BRDF of solar DUTs must be measured for a very large number of angular configurations (from a few dozen to several hundred), which

requires significant overall measurement time. However, as mentioned earlier, the ambitious target sensitivity of the CO2I instrument demands exceptional precision and accuracy in solar DUT calibration. In principle, these requirements can also be met using the absolute measurement method. Nevertheless, calibrating solar DUTs with this approach in practice will entail a significantly longer overall measurement time, making it much more expensive than the relative measurement method.

To conclude this section, it is essential to note that despite the apparent simplicity of the developed BRDF bench, it is, in practice, a rather complex and expensive measurement system. Its implementation requires significant engineering efforts along with numerous auxiliary experimental studies, the descriptions of which are omitted in this article for brevity. This article also leaves out the description of several auxiliary subsystems and components, such as the alignment system, the baffling system, and the cleaning system, which are necessary to achieve the required measurement accuracy and precision. A more detailed description of these subsystems and components can be found in our publications [9]-[11] and in our forthcoming specific papers.

4. EXPERIMENTAL RESULTS

4.1 SK light source calibration

Before proceeding with the solar DUT BRDF measurements, it is essential to calibrate the developed SK supercontinuum light source and determine the corresponding correction factors to substitute into Eq. (3). As a result, after completing its assembly and debugging, the SK supercontinuum light source underwent a series of optical tests.

Fig. 7 illustrates an example of the developed SK light source spectral calibration results.

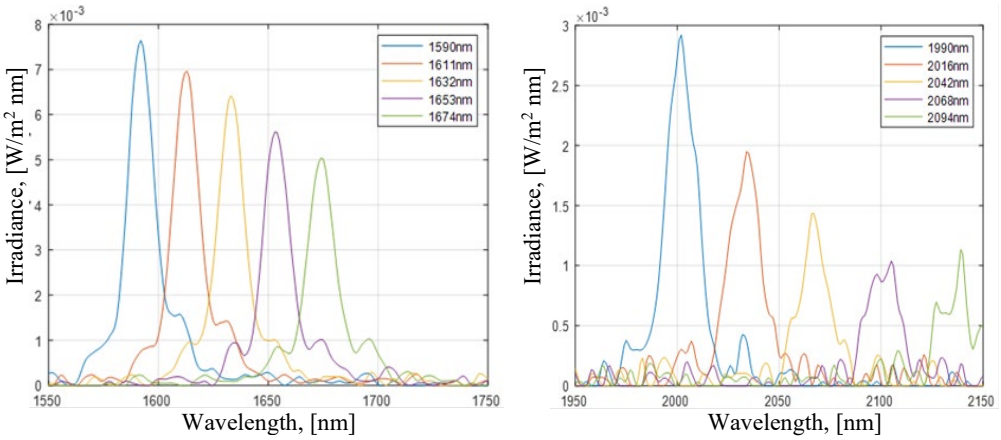

Figure 7. Results of the spectral calibration of the SK light source for SWIR-1 (left) and SWIR-2 (right) ranges

The next figure shows examples of the normalized intensity profiles of the light beam measured at the output of the developed SK light source.

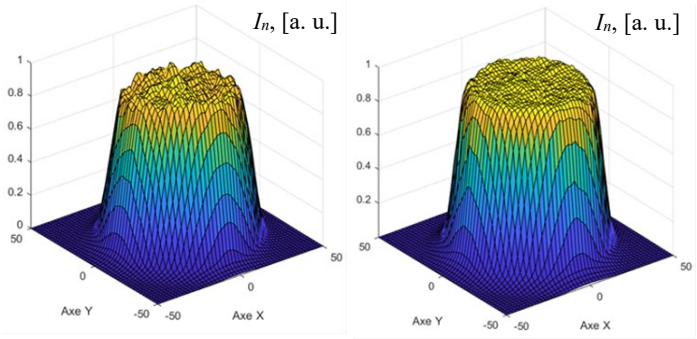

Figure 8. Source output beam uniformity measurement results for SWIR-1, λ=1632 nm (left) and SWIR-2, λ=2035.5 nm (right) spectral ranges.

The results of the light beam intensity profile measurements (see Fig. 8) are used to calculate the beam uniformity correction factor (Funif, see Eq. 3). For the sake of brevity, this article omits the description of the procedure for calculating this correction factor. Nevertheless, it is important to note that it is highly dependent on the magnitude of the incidence and observation angles (i.e., on the angular configuration for which the BRDF is measured), as well as on the operating wavelength.
The typical values of the uniformity correction factor, calculated for measurement configurations of interest as per the test specifications of the FCU project, are provided in Table 2.

Table 2. Typical values of the uniformity correction factor

Spectral band	Uniformity correction factor, F_{unif}, [a.u.]
VIS (400-500 nm)	0.9985 - 1.0121
NIR (747-769 nm)	0.9996 - 1.0069
SWIR1 (1590-1674 nm)	0.9984 - 1.0041
SWIR2 (1981-2062 nm)	0.9933 - 1.0001

In particular, in the case of the so-called 'Nominal' configuration considered in the example given in the following section, for which (θ_i, φ_i; θ_r, φ_r) = (48.57°, 9,46°, 54°, 180°), the calculated uniformity correction factor is 1.0041, 1.0031, 1.0012 and 0.9985 for the VIS, NIR, SWIR1 and SWIR2 spectral bands, respectively.

4.2 Solar DUT calibration results

In this section, we present an example of the solar DUT calibration results obtained using the developed BRDF measurement bench.

Fig. 9 shows the absolute BRDF measured in a nominal angular configuration for the Nominal (Diff1) and Redundant (Diff2) solar DUTs.

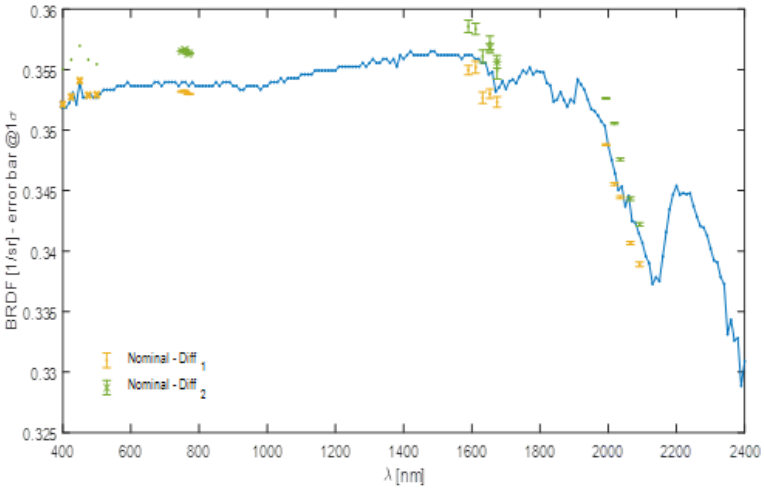

Figure 9. Absolute BRDFs of the solar DUTs measured at nominal angular configuration (θ_i, φ_i; θ_r, φ_r) = (48.57°, 9,46°, 54°, 180°). Blue line: reference sample calibration result at PTB

As noted above, according to the CO2M FCU calibration plan requirements, the BRDF of the solar DUTs must be measured for a very large number of angular configurations (up to several hundred). These measurement data are required to build an enhanced Rahman model of the solar DUT BRDF. The fitting of the angular calibration BRDF data relies on a Rahman model with 4 parameters and empirical polynomial functions (16 parameters).
An example of the BRDF Rahman model is illustrated in the next figure.

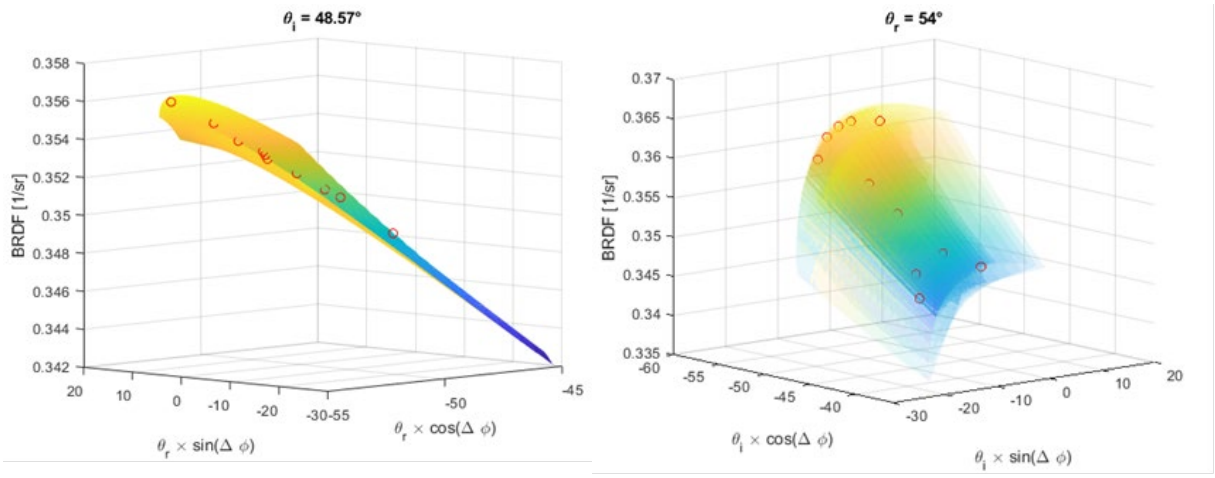

Figure 10. 3D visualization of BRDF measurement and fitting, nominal diffuser, 400 nm wavelength, (left) incidence elevation angle = 48.57° (nominal incidence angle) and (right) observation elevation angle = 54° (nominal observation angle). Colored surface: Modelled BRDF. Red circles: Measured BRDF.

Fitting performances are illustrated in the following figure. Each incident angle corresponds to a cross color.

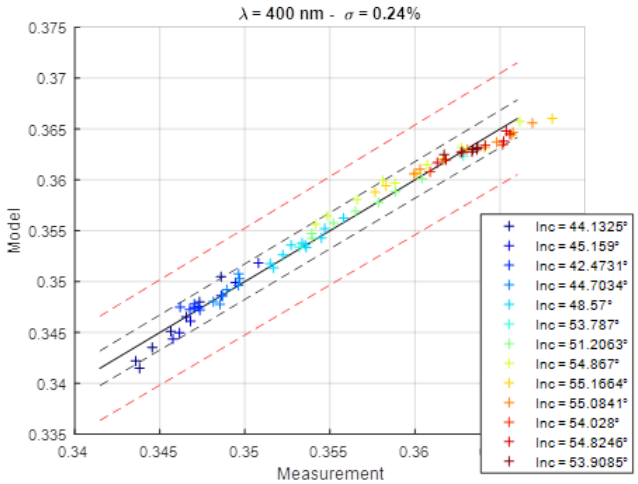

Figure 11. Comparison between model BRDF (dark solid line) and measured BRDF (crosses, one color for each incident angle) at all wavelengths for the empirical function model (Rahman). Dashed dark lines correspond to 0.5% and dashed red lines to 1.5% deviation.

The Rahman fitting model errors at 2σ-level with respect to the measured BRDF are listed in Table 3.

Table 3. Typical values of the Rahman fitting model error for the spectral bands of interest

Used light source	Spectral sub-band	Fitting model error
Xe-arc lamp source	400 nm < λ < 550 nm (VIS)	0.55%
SK supercontinuum light source	700 nm < λ < 800 nm (NIR)	0.69%
	1500 nm< λ < 1650nm (SWIR1)	1.12%
	1650nm < λ < 1700 nm (SWIR1)	1.57%
	1900 nm < λ < 2100 nm (SWIR2)	1.51%

It is instructive to note that the fitting error values provided in the table above can still be reduced by further optimizing the correction term $F'(P,k_{ij})$ of the Rahmann model (see Eq.6).
To conclude this section, it is instructive to compare the precision of BRDF measurements achieved on the presented CLS BRDF metrology bench before and after the aforementioned modification of the NIR-SWIR light source (i.e., the measurement precisions achievable with the old light source involving a Xe-arc lamp and with the new one based on a SK supercontinuum laser). The results of this comparative study are listed in Table 4.

Table 4. Absolute BRDF calibration results; total random-type errors contribution to the error budget

NIR-SWIR light source type	ε @ 2σ-level			
	NIR	SWIR1 λ <1650nm	SWIR1 λ >1650nm	SWIR2
Xe-arc lamp with dedicated filters	0.56 %	1.52 %	1.70 %	1.70 %
Supercontinuum light source	0.31%	0.54%	0.53%	0.54%

As shown in Table 4, the use of the supercontinuum light source has enabled an increase in BRDF measurement precision by a factor of two in the NIR and three in the SWIR spectral ranges, respectively.
In our experimental work, the error budget is evaluated according to the standard methodology recommended by [24]-[25]. Therefore, this paper omits details of the uncertainties analysis procedure for the sake of brevity, focusing only on the general results obtained (the main issues related to the uncertainties analysis problem will be published in a forthcoming paper).

5. CONCLUSIONS AND PERSPECTIVES

In this paper, we present an innovative instrumental platform designed to implement a high-precision approach to BRDF metrology, and we also discuss some key engineering aspects of its practical implementation.
The instrumental platform was developed based on the previous CSL BRDF robot-based goniometric bench. In particular, a new light source utilizing SK supercontinuum laser and AOTF modules was created for BRDF measurements in the infrared spectral ranges. The implementation of this new light source has enabled a significant improvement in the accuracy and precision of BRDF measurements in the NIR and SWIR spectral ranges.
The functionality of the developed characterization bench was tested and validated within the CO2M FCU project. The effectiveness of the presented instrumental approach is demonstrated by the experimental results reported and discussed in the paper.
Finally, it should also be noted that the measuring bench presented in this article was designed according to the modular principle. Accordingly, the version of the measuring bench used in the CO2M project (and thus optimized for the requirements of this project) is not the only possible configuration: if necessary, other types of optoelectronic subsystems and components can be added to the measuring bench, such as additional filters, wave plates, etc.
Regarding the future development of the presented BRDF bench, the plan includes significant improvements and extensions of its functionalities in the near future. In particular, we intend to expand the available spectral range of the BRDF bench to 4 μm by using an additional supercontinuum light source operating in the Middle-Wave Infrared (MWIR), which is currently under development. Additionally, we will redesign the VIS-NIR (400-1000 nm) section of the light source. The new design of the VIS-NIR light source will be based on a linear variable filter system (LVFS), allowing for continuous selection of the operating wavelength. Currently, the operating wavelength is selected in the VIS range using a set of conventional filters with fixed transmission wavelengths. It is also worth noting that since the LVFS output beam is unpolarized (according to the LVFS operating principle), the overall measurement duration in the NIR spectral range will be reduced by a factor of two compared to the currently used NIR light source.

ACKNOWLEDGEMENTS

This research has been performed in the frame of a contract between CSL and Thales Alenia Space France for the design and development of the CO2I Flight Calibration Unit, in the frame of the ESA Copernicus CO2M Mission, funded by the EU and ESA.

REFERENCES

[1] B. Sierk et al., “The European CO2 Monitoring Mission: Observing anthropogenic greenhouse gas emissions from space”, Proc. of SPIE Vol. 11180, International Conference on Space Optics - ICSO 2018; 111800M (2019), DOI:10.1117/12.2535941

[2] B. Sierk et al., “The Copernicus CO2Mmission for monitoring anthropogenic carbon dioxide emissions from space”, Proc. of SPIE Vol. 11852 118523M-2, International Conference on Space Optics ICSO 2020 (2021)

[3] Stover, J., "Optical Scattering: Measurement and Analysis", SPIE press book (2012).

[4] J. Moreno-Ventas et al. "ALTIUS instrument: a study of scattering effects", Proc. SPIE 12777, International Conference on Space Optics — ICSO 2022, 127771N (12 July 2023); https://doi.org/10.1117/12.2689672

[5] Domken I., Plesseria J.-Y. and Mazy E., “MSI Instrument (ESA Sentinel-2): from the diffuser procurement until the test instrument at CSL”, 26th Aerospace Testing Seminar, (2011)

[6] Mazy E., Camus F. and Chorvalli V., “Sentinel-2 diffuser on-ground calibration”, Proc. SPIE 8889 (2013)

[7] Clermont L., Mazy E., Marquet B., Plesseria, JY., “An in-flight calibration for the Earth observation instrument Sentinel-4: from design to tests”, Proc. SPIE 11116 (2019)

[8] Clermont, L. et al., "Design and tests of the sun baffle for the Sentinel-4 UVN embedded calibration assembly", Proc. SPIE 10562, International Conference on Space Optics — ICSO 2016, 1056201 (25 September 2017)

[9] J.-Y. Plesseria, I. Domken, E. Mazy et al., “Development of a BRDF Measurement Bench for Characterization of Diffuse Reflective Materials”, Proceedings of 12th European Conference on Spacecraft Structures, Materials and Environmental Testing (2012)

[10] E. Mazy et al., “Recent development in BTDF/BRDF metrology on large-scale Lambertien-like diffusers, application to on-board calibration units in space instruments”, Proc. SPIE 11056 -48 (2019)

[11] L. Clermont, C. Michel, and E. Mazy, “Performance enhancement of a BSDF test bench using an algorithm fed with laser-tracker measurements”. Proceedings of SPIE: The International Society for Optical Engineering, 11057 (2019)

[12] Clermont, L., Lallemand, E., Plesseria, J. Y., Serrano, S., and Kintziger, C., "The stray light baffle for the ARRAKIHS mission", Proc. SPIE 13092, Space Telescopes and Instrumentation 2024: Optical, Infrared, and Millimeter Wave, 130923O (23 August 2024); https://doi.org/10.1117/12.3021043

[13] Clermont, L *et al.* Unlocking stray light mysteries in the CoRot baffle with the time-of-flight method. *Sci Rep* 14, 6171 (2024). https://doi.org/10.1038/s41598-024-56310-z

[14] Montanaro, M. et al. Performance of the proposed stray light correction algorithm for the Thermal Infrared Sensor (TIRS) onboard Landsat 8. Proc. SPIE 9972, 99720F (2016)

[15] Montanaro, M. et al. Toward an operational stray light correction for the landsat 8 thermal infrared sensor. Appl. Opt. 54(13), 3963–3978 (2015).

[16] Laherrere, J.-M., Poutier, L., Bret-Dibat, T., Hagolle, O., Baque, C., Moyer, P., & Verges, E. POLDER on-ground stray light analysis, calibration, and correction. In Proceedings of SPIE 3221, Sensors, Systems, and Next-Generation Satellites, (1997) https://doi.org/10.1117/12.298073

[17] Clermont, L., C.Michel, Chouffart, Q. et al. Going beyond hardware limitations with advanced stray light calibration for the Metop-3MI space instrument. Sci Rep 14, 19490 (2024). https://doi.org/10.1038/s41598-024-68802-z

[18] Clermont, L.; Michel, C.; Stockman, Y. Stray Light Correction Algorithm for High Performance Optical Instruments: The Case of Metop-3MI. Remote Sens. 2022, 14, 1354. https://doi.org/10.3390/rs14061354

[19] Clermont, L., Michel, C., Mazy, E., Pachot, C., Daddi, N., Mastrandread, C., and Stockman, Y., "Stray-light calibration and correction for the MetOp-SG 3MI mission", Proc. SPIE 10704, Observatory Operations: Strategies, Processes, and Systems VII, 1070406 (10 July 2018); https://doi.org/10.1117/12.2314208

[20] Clermont, L, Michel, C., "Out-of-field stray light correction in optical instruments: the case of Metop-3MI," Journal of Applied Remote Sensing 18(1), 016508 (4 March 2024). https://doi.org/10.1117/1.JRS.18.016508

[21] Fest, E. Stray Light Analysis and control (SPIE Press, Bellingham, 2013). https://doi.org/10.1117/3.1000980.

[22] Plesseria, J.Y., et al., "Utilisation of acktar black coatings in space applications," International Symposium on Materials in the Space Environment (2018).

[23] H. Rahman et al., “Coupled surface-atmosphere reflectance (CSAR) model. Model description and inversion on synthetic data”, Journal of Geophysical Research, Vol. 98, D11, pp.20779-20789 (1993)

[24] B.N. Taylor and Ch. E. Kuyatt, “Guidelines for Evaluating and Expressing the Uncertainty of NIST Measurement Results”, NIST Technical Note 1297, 1994 Edition, NIST, National Institute of Standards and Technology, (1994)
[25] K. Birch, “Measurement Good Practice Guide No. 36. Estimating uncertainties in testing”, British Measurement and Testing Association, UK, (2003)